Experimental Test of the Conservation of Nucleons*

C. C. GIAMATI† AND F. REINES‡
Case Institute of Technology, Cleveland, Ohio
(Received February 1, 1962)

An improved measurement has been made of the lower limit for the lifetime of nucleons against spontaneous decay by processes which do not conserve the number of nucleons. The decay modes considered release charged particles with energies generally in excess of 100 Mev. Possible decay events were sought with a 200-liter liquid scintillation detector. Backgrounds were due entirely to cosmic rays which were reduced by going 585 m underground and then surrounding the scintillation detector by a water Čerenkov anticoincidence counter of over-all dimensions 2.4 m in diameter and 2.0 m high. The scintillation detector was set to detect pulses as low in energy as 8 Mev and hence was sensitive to a wider variety of decay events than previous experiments. Lifetime limits obtained range from 1×10^{26} to 7×10^{27} years depending on the decay mode assumed.

INTRODUCTION

THE law of conservation of nucleons was proposed by Stückelberg[1] and Wigner[2] as a statement that the number of nucleons, counted algebraically, remains constant. This statement was first made to explain the stability of matter, and was later generalized to include baryons. Such a conservation law is perhaps more suspect than those for energy, momentum, and parity, which can be related directly to symmetry principles.[3–5] The experiments dealing with the nonconservation of parity in weak interactions have reminded us of the value of testing conservation laws in even more varied and stringent ways, and it is for this reason that the present experiment was performed.

In considering possible modes of decay we observe that if the conservation laws of energy, momentum, spin, charge, and lepton number are assumed to be valid, then nucleon conservation is required since the production of any known particles requires the violation of at least one conservation law in addition to that for nucleon conservation. Here we assume the breakdown of lepton conservation since it is the least well founded and hence least objectionable violation to be associated with nucleon nonconservation.[6]

The degree to which the law of conservation of nucleons is valid is usually expressed as a limit on the lifetime of nucleons. The first explicit experiment designed to investigate lifetime limits was performed by Reines, Cowan, and Goldhaber,[7] who looked for possible decay events in 300 liters of liquid scintillator located 60 m underground and found for nucleons bound in nuclei $\tau>10^{22}$ years. A later experiment by Reines, Cowan, and Kruse[8] in which a delayed coincidence was sought between the energetic charged product particle and the capture of a product neutron gave a value $\tau>4\times10^{23}$ years for protons bound in deuterons. Higher limits on nucleon lifetimes were obtained by Backenstoss *et al.*[9] who used the directional properties of a counter array including a Čerenkov detector to look for relativistic charged particles emerging from matter beneath the counters. Background due to natural radioactivity was eliminated by requiring an energy deposition greater than 5.0 Mev in one counter, accompanied by a relativistic particle in another counter. Cosmic rays were discriminated against by performing the experiment 800 m below rock, and looking only at particles traveling upward. No events attributable to nucleon decay were observed in 265 hr. Three separate runs were made with the counters over water, lead, and the rock floor. The limits obtained in this experiment were calculated by assuming a kinetic energy of 250 Mev to be available to one particle which was taken to be either a photon, positron, muon, or pion. Using the range of the charged products and the pair production cross section for the photons and correcting for radiation loss and nuclear interactions, the relationship between an upward flux through the counter system and a nucleon decay rate was calculated. The limits obtained were $\tau>4.7\times10^{24}$ years for protons in hydrogen, $\tau>4.3\times10^{25}$ years for protons in lead, and for the three combined runs $\tau>2.8\times10^{26}$ years for all nucleons.

The present investigation of nucleon stability was made with a detector system differing in several respects from those used previously. In the present measurement we looked for events depositing more than 8 Mev in a 200-liter liquid scintillation detector, unaccompanied by an event in a large cosmic-ray anticoincidence Čerenkov counter which blanketed the top and

* Supported in part by the U. S. Atomic Energy Commission.
† Now at Lewis Research Laboratory, National Aeronautics Space Administration, Cleveland, Ohio. Work performed while on leave at Case Institute under the NASA graduate study program.
‡ Alfred P. Sloan Fellow.
[1] E. C. G. Stückelberg, Helv. Phys. Acta. **11**, 225, 299 (1938).
[2] E. P. Wigner, Proc. Am. Phil. Soc. **93**, 521 (1949); Proc. Natl. Acad. Sci. U. S. **38**, 449 (1952).
[3] G. C. Wick, Ann. Rev. Nuclear Sci. **8**, 1 (1948).
[4] G. Feinberg and M. Goldhaber, Proc. Natl. Acad. Sci. U. S. **45**, 1301 (1959).
[5] M. A. Melvin, Revs. Modern Phys. **32**, 477 (1960).
[6] Nucleon conservation on the other hand does not imply lepton conservation. Nor would the lack of lepton conservation necessarily lead to nucleon nonconservation.
[7] F. Reines, C. L. Cowan, Jr., and M. Goldhaber, Phys. Rev. **96**, 1157 (1954).
[8] F. Reines, C. L. Cowan, Jr., and H. W. Kruse, Phys. Rev. **109**, 609 (1957).
[9] G. K. Backenstoss, H. Frauenfelder, B. D. Hyams, L. J. Koester, Jr., and P. C. Marin, Nuovo cimento **16**, 749 (1960).

sides of the liquid scintillation detector. The lower limit 8 Mev was chosen to eliminate natural radioactivity as a source of background. Events which might occur in the inner detector were prevented from tripping the anticoincidence counter by 7.4 metric tons of steel shielding placed around the internal detector, effectively isolating it from the anticoincidence counter for the energies possible in nucleon decay events. The cosmic-ray background was reduced by a factor of 4×10^4 from that at sea level by placing the entire assembly in a salt mine 585 m underground.

The following two sections of the paper describe the experimental equipment; the first relating to design and construction, the second to calibration and use. The final two sections give the experimental results and an analysis. An Appendix contains details relevant to calculations of the lifetime limits.

EQUIPMENT DESIGN AND CONSTRUCTION

Liquid Scintillation Detector

The liquid scintillation detector was a stainless steel tank in the form of a right circular cylinder 60.5 cm in diameter and 72 cm high. The tank and cover were sandblasted and painted with a white epoxy base paint (Plasite) to obtain good reflectivity from the inner surfaces and to provide a clean container for the liquid scintillator. The steel tubings, in which the phototubes were housed, were sealed on their lower ends by clear plastic discs cemented with an epoxy adhesive. After filling the tank with the liquid scintillator, the cover was sealed permanently with epoxy cement. The schematic diagram in Fig. 1 shows this detector as well as the entire assembly, which was placed in the salt mine.

The tank was filled to a depth of 69 cm with 200 liters of liquid scintillator which was prepared by adding 0.8 g/liter of *p*-terphenyl and 1.5 g/liter of α NPO to the solvent Decalin[10] (decahydro-naphthalene). The choice of the solvent was dictated in part by safety regulations at the final experimental site in the salt mine.

The four photomultiplier tubes were Dumont type 6364 (nominal 5-in.-diam photocathode) which were selected from a group of 112 to have approximately the same gain and resolution, and to be free from excessive noise. The gain of each tube was then balanced by means of a resistor inserted in series with the standard voltage divider network.[11] The tubes were optically coupled with Dow-Corning silicone jelly to the plastic windows which were immersed directly in the liquid. Each tube had individual signal and high-voltage cables leading outside the tank assembly, so that in case of a photomultiplier tube failure the experiment could be continued without dissassembling the system. In this experiment, tubes numbered 1 and 3 were used as one unit designated as I, and tubes numbered 2 and 4 as a second unit II.

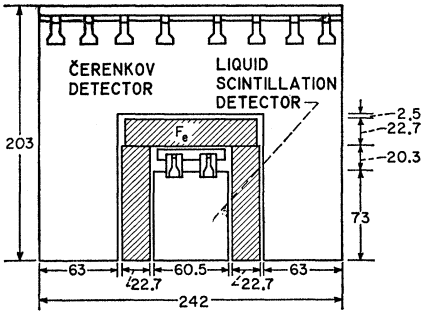

FIG. 1. Schematic diagram of the detector system. All dimensions in centimeters.

Steel Shielding

The scintillation detector was surrounded on the top and sides by a minimum of 22.8 cm of steel (99.4% Fe). The steel was in the form of 3-in. square billets, in lengths of 29, 32, and 35 in. stacked so the sides formed a hollow rectangular shell 12 billets high and 3 billets thick. Three layers of 12 billets each 36 in. long, were stacked in place to form the top. The shield thickness was chosen so that less than 10% of the most energetic muons originating from a possible decay of a nucleon at the inner wall of the scintillation detector could penetrate the shield. Even the most energetic nucleon decay muon would be degraded in energy by the minimum shield thickness so that the probability of creating a detectable pulse in the anticoincidence Čerenkov counter was negligible.

Anticoincidence Counter

The anticoincidence Čerenkov counter was formed from a right circular cylinder of sheet iron 2.4-m inside diameter and 2.0 m high. The walls of the tank consisted of four semicircular pieces bolted together against rubber gaskets and to a circular floor plate. An insert in the form of an inverted can was bolted over an opening in the bottom plate to complete the tank assembly. This construction was used in order to permit the sections to be lowered to the salt mine floor through an access shaft. White plasite was applied to the entire tank before assembly and served to enhance the reflectivity of the inner walls and inhibit corrosion. The tank was capped by a plywood cover in which 52 Dumont type 6364 photomultiplier tubes were mounted to view the liquid in the tank. The tube faces were immersed to a depth of about 3 cm. This method of mounting the tubes was chosen for ease of construction and to avoid the problem of leaks in window seals which might occur in photomultiplier tube housings inserted into the sides or bottom of the tank. The occurrence of leaks would be especially serious during the measurements underground

[10] C. L. Cowan, Jr., Catholic University Progress Report, 1959 (unpublished).

[11] F. Reines, C. L. Cowan, Jr., F. B. Harrison, A. D. McGuire, and H. W. Kruse, Phys. Rev. **117**, 159 (1960).

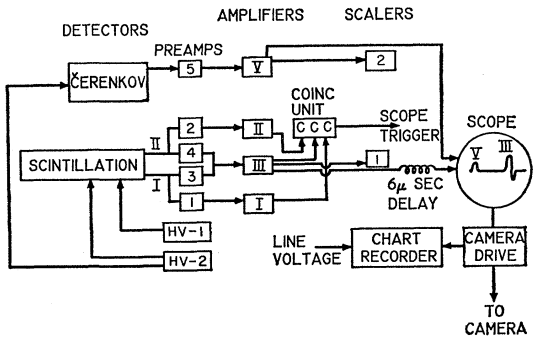

FIG. 2. Block diagram of the electronics system.

when the equipment was inaccessible because of the mine operating schedule for periods of $2\frac{1}{2}$ days every week. The city drinking water used for the Čerenkov medium was passed through a silica gel filter and two tandem demineralizing resin exchange beds prior to flowing into the tank. At each filling 7200 liters of water were used, and 35 g of β-methyl umbelliferone were added as a wavelength shifter.[12]

Individual photomultiplier tubes were balanced to have equal gains by insertion of a gain balance resistor between the common high-voltage yoke and the voltage divider network, and the signal outputs were added just ahead of a common preamplifier. The tubes were tested for noise and approximate gain prior to insertion in the tank both at Case Institute and again at the salt mine.

Electronics

A block diagram of the detectors and associated electronics is shown in Fig. 2. The linear amplifiers were of the ORNL A-8 type with built in pulse-height discriminators giving two shaped triggered pulse outputs as well as the direct amplifier output. By way of illustration we describe how the system represents a cosmic ray passing through both tanks. In the liquid scintillation detector, signals from photomultiplier units I and II are sent through their respective preamplifiers directly to amplifiers I and II, and a sum signal is sent to amplifier III. When the signals from the three amplifiers exceed set thresholds (8 Mev in amplifier III) pulses are sent to the coincidence unit. A threefold coincidence ($2t=2$ μsec) triggers a 10-μsec oscilloscope sweep. The sum pulse from amplifier III is delayed 6 μsec and displayed on the oscilloscope. The signal from the anticoincidence counter is sent to amplifier V, and when this signal exceeds a set threshold, a shaped pulse is displayed on the oscilloscope at the beginning of the sweep. The oscilloscope trace shown schematically in Fig. 2 is photographed by a 35-mm camera which remains with shutter open at all times. The oscilloscope sweep circuit furnishes a trigger pulse to drive a relay unit which actuates the camera drive to advance the film and at the same time puts a marker blip on the chart paper of an Esterline-Angus recording voltmeter. The spring drive recording voltmeter serves as a monitor for the power line voltage and a means of recording the absolute time at which an event occurred in the inner tank.

[12] N. A. Porter, Nuovo cimento 5, 526 (1957).

EQUIPMENT CALIBRATION AND USE

Liquid Scintillation Detector

The energy scale for the scintillation detector was established by the peak in the spectrum as seen at Case Institute due to those cosmic rays which passed through the detector. First, each of the four photomultiplier tubes viewing the scintillator was adjusted to give a chosen gain by measuring a cosmic-ray energy spectrum using the signal from one tube at a time, and adjusting the high voltage on each tube until the through peak fell in the same channel of a T.M.C. 256-channel pulse-height analyzer (PHA.). The sum pulse spectrum (amplifier III) was measured on the PHA. and the through peak channel noted. Immediately before and after this measurement a pulse generator calibration was measured with the PHA. so that the cosmic spectrum as seen by the detector was related to the pulse generator dial settings. The through peak energy 116 Mev was calculated from the average depth of the liquid in the tank assuming an energy deposition of 1.6 Mev/cm for minimum ionizing particles, and adding a 5% correction for fluctuations in energy loss and the angular distribution of the cosmic rays. The cosmic-ray spectrum is shown in Fig. 3 along with the pulse generator calibration line. Over a period of 36 days there was an upward drift in the through peak of less than 2.5%. The high-voltage supplies were turned on and off irregularly after this period, but two measurements taken a few weeks and again a month later, just prior to moving the detector to the salt mine, showed a drift upward of less than 1.4% in the through peak.

The energy calibration of the scintillation detector in the mine was carried out following the same principle used on the surface but because of the lowered cosmic-ray count rate in the mine the pulse-height analysis was made by measuring the pulse height on photographs

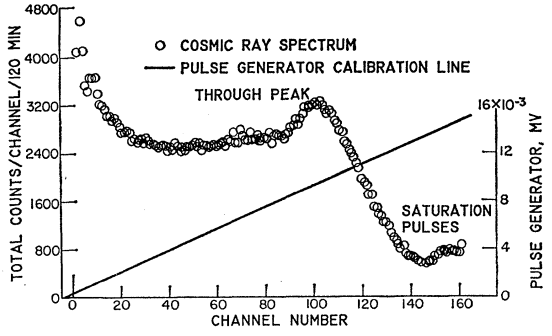

FIG. 3. Cosmic-ray spectrum in scintillation detector as measured at ground level with a multichannel analyzer.

TABLE I. Lower gate energies.

Assumed peak position (cm)	Pulse generator dial setting (v)	Lower gate (Mev) energy at dial 0.60×10^{-3}
Underground		
2.2	8.2×10^{-3}	8.5
2.4	9.0×10^{-3}	7.7
2.6	9.7×10^{-3}	7.2
Above ground	9.3×10^{-3}	7.5

of the oscilloscope traces taken during the actual data runs rather than by means of the PHA. During a period of 30 days about 2300 traces were recorded at gain settings such that a full spectrum could be measured. During the same period about 1700 other traces were recorded at different gain settings. The second group of traces was not used for purposes of calibration. The spectrum determined from the oscilloscope photographs is shown in Fig. 4, and it gives a through peak which lies in the range 2.2 to 2.6 cm. The lower gate was always reset using the same pulse generator voltage which corresponded to a nominal energy of 7.5 Mev as determined from the spectrum taken above ground. Table I shows the lower gate energy for three assumed positions of the through peak, and the pulser settings corresponding to these positions as well as the pulser setting for the through peak measured above ground. It is believed that no large drifts occurred in the system because: (a) The total spectrum accumulated over 30 days in the mine is roughly the same as the spectrum accumulated over 30 min at the surface. This is shown in Fig. 5 where the solid line represents the spectrum of the cosmic rays above ground, and the individual points, measured underground, are normalized to agree with the curve in the vicinity of the through peak. Since the angular distribution of muons underground and at the surface are different (the cosmic-ray muon intensity falls off as $\cos^2\theta$ at the surface and approximately as $\cos^3\theta$ underground,[13] where θ is the azimuthal angle), precise agreement is not expected; (b) during the runs in the mine a check on the stability of the system was made at 2- or 3-day intervals by noting the variation in the lower sum gate setting necessary to give a fixed count rate from a Cs^{137} source which was inserted under the detector; (c) a comparison (Fig. 6) of the cosmic-ray spectra for two runs taken three weeks apart showed the pulse height where the maximum counts accumulated, to be at 2.7 cm indicating a maximum difference of 8%; (d) drifts of less than 2.5% had been observed over longer running times and for much better statistics during tests on the surface and it seems reasonable to assume no significant change in the detector characteristics during the transfer to the mine.

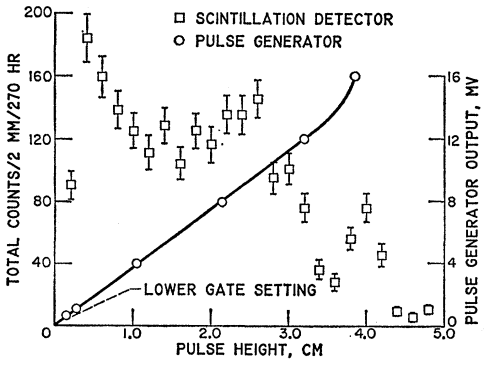

FIG. 4. Total spectrum in scintillation detector as measured underground with oscilloscope photographs during a 30-day period.

[13] P. H. Barrett, M. Bollinger, G. Cocconi, Y. Eisenberg, and K. Greisen, Revs. Modern Phys. 24, 133 (1952).

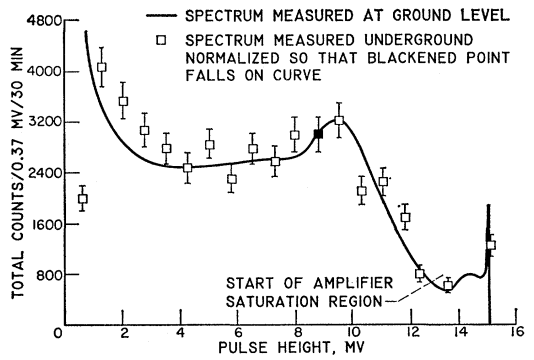

FIG. 5. Comparison of cosmic-ray spectrum in scintillation detector as measured at ground level with spectrum measured underground.

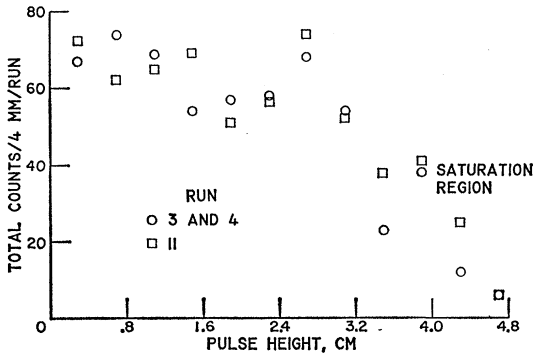

FIG. 6. Comparison of two cosmic-ray spectra in scintillation detector as measured underground 3 weeks apart.

Anticoincidence Counter

During the period of operation in the mine, a record of the integral count rate for the Čerenkov counter above an arbitrary level showed a drift of about 5% during 3 weeks and a drift of about 20% during a period of a week when the air conditioning unit failed partially and allowed the temperature in the electronics shed to rise to 90°F from a normal 78°F. This rate was taken with the gate level at an energy such that noise pulses were being counted and, hence, because the noise spectrum was rising steeply with decreasing energy, the

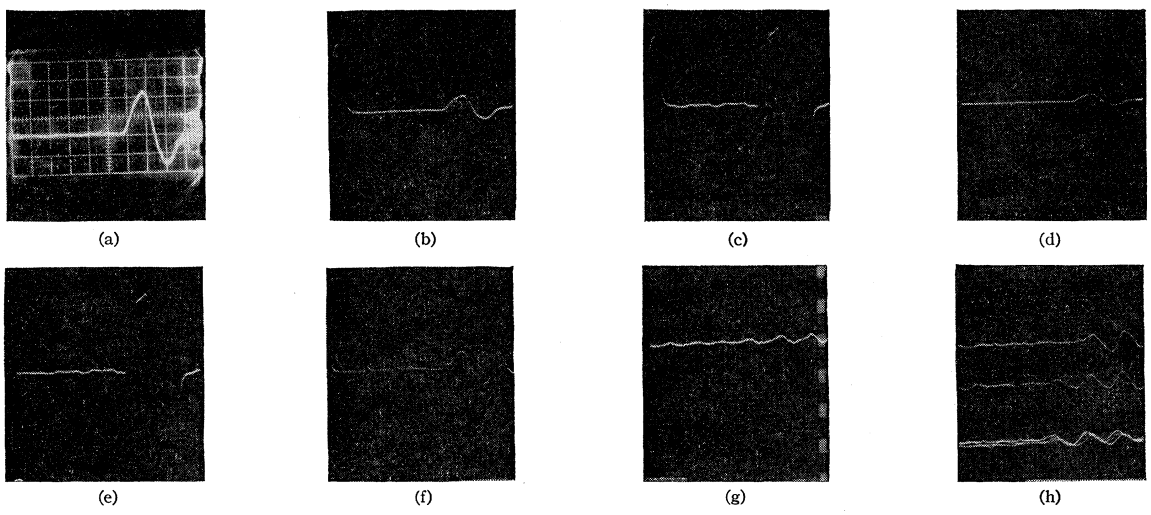

FIG. 7. Typical oscilloscope traces. The sweep speed is 1 μsec/cm. The left-hand pulse at the beginning of the sweep is the Čerenkov pulse. The scintillation detector pulse is delayed 6 μsec with respect to start of sweep. (a) Calibration trace from pulse generator. (b), (c) Cosmic-ray events. (d) Scintillation pulse of 12-Mev energy unaccompanied by a Čerenkov pulse. (e) Scintillation pulse of energy greater than 150 Mev unaccompanied by a Čerenkov pulse. (f), (g), (h) Noise pulses.

variation in gate setting for the 20% drift in integral rate was less than 10%.

The water available underground prior to filtering and demineralizing contained more organic material and oil traces than did the water available at Case Institute. Thus the filtered and demineralized water used in filling the tank underground was not as clear and transparent as the water used previously. Visual inspection of the tank after filling underground showed a noticeably murkier appearance than that of the water obtained above ground. It was found that when using the same gain settings for the anticoincidence system as used on the surface about 1/20 of the pulses in the scintillation tank were unaccompanied as compared with an anticoincidence factor measured above ground of several hundred. This supported the idea that the Čerenkov tank light output and hence its efficiency for detecting particles using a given amplifier gain was much lower than before. Since no cleaner water was available in a reasonable time, the amplifier gain was raised by a factor of 2. This change raised the signals due to cosmic rays to an acceptable level and, as demonstrated by subsequent measurements, the Čerenkov detector served as an effective anticoincidence shield.[14]

Electronic Stability

The stability of the electronics was checked by using the pulse generator to make all gate settings, and then referring the dc level of a test point on the pulse generator to a Simpson voltmeter. This reference voltage was a nominal 83 v, and no departure of more than 0.5 v was seen at any time, so that the pulse generator voltages were stable within pulse or minus 0.6%. An additional check on the stability of the pulse generator was obtained incidental to the measurements taken with the pulse-height analyzer since a calibration curve was measured each time. The channel in which a pulse of 8×10^{-3} v fell varied by one channel out of 91 during all the measurements on the surface and in the mine. It is possible that any drift in the pulse generator was compensated by a drift in the analyzer, but since the pulse generator was left on continuously and the portable analyzer was moved and turned on just prior to the measurements which varied in length from a few hours to a few days, with calibrations taken at intervals during the measurements, such an accidental compensation in every case does not seem likely. While in the mine the electronics equipment and camera were housed in a wooden cubicle 3.3 m on a side for protection from the environment. An air conditioner was provided for temperature and humidity control, and to filter dust and salt particles from the incoming air.

EXPERIMENTAL RESULTS

Each 100-ft roll of oscilloscope record film was scanned first to determine the number of traces in each category and then to measure the pulse-height spectrum. The traces could be grouped as follows: cosmic rays, where an anticoincidence pulse and a scintillation detector pulse appeared at the proper position and the base line was otherwise smooth; unaccompanied events, a scintillation detector pulse without an anticoincidence pulse and with a smooth base line; noise pulses, traces with sharp spikes on the base line and/or scintillation pulse absent; series noise pulses, groups of noise pulses following sequentially in short time periods. Figure 7

[14] This detector is described in a paper by F. Reines and C. C. Giamati at the IAEA meeting on Nuclear Electronics held in Belgrade in May, 1961. Further details are given in the Ph.D. thesis of C. C. Giamati, Case Institute of Technology, 1962 (unpublished).

shows typical oscilloscope photographs of traces. Table II gives a summary of the results from 12 rolls of film.

Eighteen unaccompanied events were observed in 421 ± 1.5 hr.[15] All but two of these unaccompanied events were of an energy below 12 Mev; both appeared on Roll No. 12 and were overload pulses, or greater than 150 Mev. The remaining 16 events were distributed as follows: one of 5 Mev, twelve of 9 Mev, and three of 12 Mev. Because of the previously noted sensitivity of the anticoincidence factor to amplifier gain it is suspected that the unaccompanied events are due to cosmic rays which penetrated the anticoincidence shield without causing it to respond.

No dead time or coincidence corrections were necessary in the liquid scintillation detector system because the singles counting rate from photomultiplier units I and II were 800/hr and 2400/hr, respectively, and the resolving time was about 1 μsec: The calculated accidental coincidence rate is one event in 800 hr. In addition, the scintillation detector pulse rate due to cosmic rays was about 10/hr and the anticoincidence counter rate was about 3.6×10^5/hr implying negligible system deadtimes.

CONCLUSIONS

Lifetime Limits

In order to compute a lower limit for the lifetime of nucleons from the experimental results, it is necessary to make some assumptions about possible nucleon decay modes. The nucleon is assumed to decay with a lifetime τ, and the laws of conservation of energy, momentum, spin, and charge are assumed to hold for every mode.

TABLE II. Types of oscilloscope traces in underground measurements.

Roll No.[a]	Total frames	Total hours	Number of unaccompanied events	Number of noise traces	Number of series noise traces
2	178	22:00	0	5	0
3	316	34:30	2	2	0
4	279	24:35	2	11	0
5	62	6[b]	0	0	0
6	38	4:15	0	1	0
7	341	35[b]	4	6	0
8	264	25:20	0	0	0
9	486	52:30	1	9	0
10	235	25:20	1	5	12 (3 groups)
11	598	60:50	1	4	4 (2 groups)
12	643	64[b]	2,2[c]	4	23 (3 groups)
15	625	67:00	3	9	3 (1 group)

[a] Rolls Nos. 1, 13, and 14 unusable because of wrong gain settings or malfunctions in camera drive and film processing.
[b] Time estimated to nearest half hour—film roll used up.
[c] These two events were greater than 150 Mev, all others were less than 12 Mev.

[15] The uncertainty in time arises because the camera drive system failed once in such a manner as to take up all the film within a few minutes of the failure, and because on two other occasions all the film was taken up during the course of a data run over a weekend. In all these cases the running time recorded on the film had to be estimated.

TABLE III. Lower limits on nucleon lifetimes for specified decay modes.

Assumed decay mode	Lifetime limits in units of 10^{26} years[a] Free protons	Bound nucleons
$p\rightarrow\pi^++\nu$	1.5	40
$p\rightarrow K^++\nu$	1.5	10
$p\rightarrow e^++\gamma$	1.5	45
$p\rightarrow\mu^++\gamma$	1.5	65
$p\rightarrow\mu^++\nu+\bar{\nu}$	1.5	30
$n\rightarrow\pi^++e^-$		70
$n\rightarrow\mu^++K^-$		35
$n\rightarrow\mu^++e^-+\bar{\nu}$		30

[a] The limits are rounded to the nearest 5.

Chosen within these restrictions are the typical two- and three-particle decay modes listed in Table III. We considered only those modes leading to at least one charged particle since such decay events could be detected by the experimental apparatus with an efficiency approaching 100%. The nucleons are divided into three categories, (a) free protons, i.e., protons in hydrogen which are bound only by molecular electronic binding forces, (b) bound protons, i.e., the protons in the decalin nuclei, and also in the shielding iron nuclei, (c) the neutrons in the decalin and iron nuclei. Additional assumptions are necessary for each of these categories before the lifetimes can be computed and these assumptions, along with the calculational methods, are detailed in the Appendix. The lower limits for the lifetimes in each case are tabulated in Table III.

It is, of course, possible to consider decay modes in which more than three particles are created, or modes in which the conservation of energy, momentum, spin, and charge may be violated. In order to compare the present results to those of Backenstoss *et al.*,[9] additional calculations were made based on the assumptions that:

(a) A nucleon decays with a lifetime τ and gives one charged decay product or one photon.

(b) A kinetic energy of 250 Mev is available to one particle.

(c) The charged decay products are assumed to be either positrons, muons, or pions.

These limits are listed in Table IV.

TABLE IV. Lifetime limits based on decay modes leading to emission of charged particles or photons with a kinetic energy of 250 Mev.[a]

Assumed decay products	Lifetime limits in units of 10^{26} years Free protons	Bound protons	All nucleons
Muons	1.5	30	70
Electrons	1.5	20	45
Photons	1.5	20	45
Pions	1.5	30	65

[a] Assumptions of Backenstoss *et al.*[9]

In addition to these general assumptions some particular ones are necessary to take account of the specific experimental arrangement. The free-proton lifetime can be computed from the number of such protons inside the liquid scintillation detector after making a slight reduction to correct for edge effects. This correction is made by computing the fraction of all possible paths traversed by decay products which are shorter than 5 cm, the minimum path necessary to give a detectable signal. A similar computation gives as 0.06 the fraction of possible paths which give rise to signals corresponding in energy to the range 8 to 12 Mev.

The observed count rate of 16 counts in the energy range 8 to 12 Mev and two counts of energy greater than 150 Mev is not consistent with this estimate. If the two counts of high energy are accepted as decay counts it is probable that only 6% (or 1) of the observed counts are decay counts in the energy range 8 to 12 Mev. Thus a decay count rate of two high-energy counts plus one low-energy count or a total of three counts is taken for purposes of computing the lifetime limits for the cases where the only energy requirement is that more than 8 Mev be released in the scintillation tank.

The computation of lifetimes for the bound protons introduces an additional assumption. The contributions from the shield can be estimated by replacing the actual detector and shield geometry by an equivalent spherical detector and a spherical shell shield. The number of bound protons in the shield which can contribute to a detectable signal pulse can be found by considering the percentage of paths traversed by decay products having a range less than the maximum range of the particle with specified kinetic energy. The total number of particles which can contribute to the detectable decay process is then obtained by adding those in the liquid scintillator to those in the shield. The same procedure is used to make estimates for neutrons and the arguments against including all 16 of the observed low-energy counts in the decay count rate which were used previously are again applicable to these cases.

Remarks

The lifetime limits obtained on the basis of the general assumptions of Backenstoss *et al.*[9] are about the same as those we compute for some plausible specific decay modes. These limits are an order of magnitude greater than those previously published, and were obtained under different experimental conditions. This means that the lifetime limits are not sensitively dependent on the specific decay modes.

The observed counts cannot be uniquely attributed to nucleon decay since only two large pulses were seen, and as discussed above these could also be due to cosmic rays.[16] Since the anticoincidence shield was not at its maximum efficiency when set up in the mine due to relatively opaque water, speculation is best postponed until an improved experiment can be done. Yamaguchi[17,18] has conjectured that the true lifetime of matter may be near the limits given by Reines, Cowan, and Kruse,[8] that is, near 10^{23} years. The limits set by Backenstoss *et al.*[9] and more stringently here indicate that Yamaguchi's conjecture is an underestimate of the true lifetime of matter.

[16] Such pulses could also be produced by energetic neutrinos.

APPENDIX. CALCULATION OF LIFETIMES FOR VARIOUS DECAY MODES

Factors in Estimating Lifetimes

Possible decay modes.—The decay modes considered are listed in the first column of Table III. The possible decay modes for protons can be separated into those which give a unique energy to the charged particles, and those which give a spectrum of energies. The lifetimes for modes giving a unique energy will be considered first.

The lifetime for an assumed proton decay process when a count rate $\Delta N/\Delta t$ is observed can be calculated using the relation

$$\tau=0.69N/(\Delta N/\Delta t), \qquad \text{(A1)}$$

where N is the number of protons available for the decay process. If only protons in hydrogen (free protons, bound only by a few electron volts in the hydrocarbon molecules) are assumed to decay the number of protons effective for decay is just the number of hydrogen atoms in the liquid scintillator reduced by a small factor to allow for events occurring so near the tank walls that less than 8 Mev might be deposited. If protons bound in nuclei are assumed to decay, then some fraction of the shielding iron atoms become effective and a contribution from these must be added to the number of protons in the tank in order to compute a lifetime limit.

Equivalent detector and shield.—The volume correction factors depend on the ranges of the charged particles and hence on their energies. Since the real geometry of the detector liquid and shielding as shown in Fig. 8 is

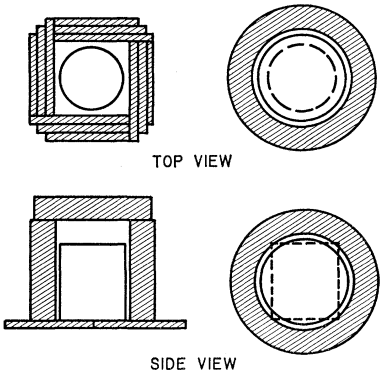

FIG. 8. Scintillation detector and shield geometry. The actual geometry is at left, the equivalent geometry at right, with dashed lines showing actual detector.

[17] Y. Yamaguchi, Progr. Theoret. Phys. (Kyoto) **22**, 373 (1959).
[18] Y. Yamaguchi, Suppl. Progr. Theoret. Phys. (Kyoto) **11**, 1 (1959).

more complicated for the purpose of calculating such factors than is warranted by the data, a simple geometry can be chosen to approximate the actual situation.

This equivalent geometry is shown in Fig. 8 where the detector is replaced by a sphere, and the iron shield by a spherical shell 22.9 cm thick, with a small air gap between them.

The radius of the equivalent detector sphere was chosen on the basis of surface area as follows. From points close to the detector walls (i.e., distances small compared to the dimensions of the detector) the surfaces can be approximated by planes. Hence the equivalent sphere for these near points can be taken as that sphere with surface area equal to the area of the cylinder. This equivalent sphere radius is 38.7 cm. From points very far from the walls, the area seen normal to the line of sight can be expressed as

$$A(\theta)=bh\sin\theta+\pi b^2\cos\theta, \tag{A2}$$

where b is the cylinder radius, h its height, and θ the azimuthal angle of spherical coordinates with the polar axis along the cylinder axis. The effective area seen from all points equidistant from the center of the cylinder can be obtained by integrating over the solid angle. The equivalent sphere radius is obtained by noting that for the sphere the area normal to the line of sight is always πr_s^2, so that the effective area can be set equal to the effective area of the equivalent sphere,

$$2\pi\int_0^{\pi} A(\theta)\sin\theta d\theta=4\pi(\pi r_s^2). \tag{A3}$$

The equivalent sphere radius for distant points is found to be 48.7 cm. Thus the equivalent sphere radius lies in the region $38.7<r_s<48.7$. The iron shield is 22.9 cm thick so that even the most distant points of the equivalent shell are points relatively close to the detector, hence the "close" case is more likely to be the better approximation. A value of $r_s=40$ cm was taken as a conservative choice, i.e., one which leads to an underestimate of the lifetimes.

An air gap of 5 cm, equal to the real air gap of the side walls was chosen and a shield thickness of 22.9 cm, equal to the real shield thickness was used. The weight of the equivalent shield was computed as 7.3 metric tons as compared to the real shield weight of 7.4 metric tons. The 5-cm air gap thus allowed both the equivalent shield mass and thickness to be nearly equal to the real mass and thickness.

Calculation of Proton Lifetime

Free proton.—In order to calculate the number of free protons inside the tank which can be effective for the decay processes, a correction must be made for those protons near the tank walls whose decay might give rise to a charged particle traveling in a direction so as to deposit less than 8 Mev in the liquid scintillator, and

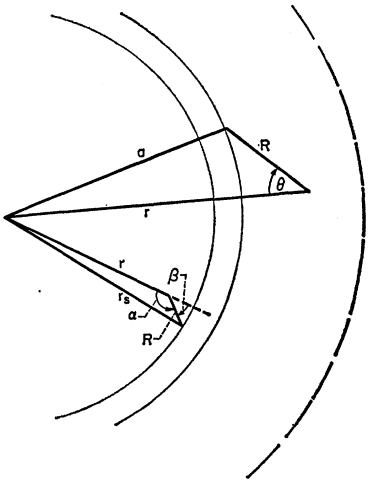

FIG. 9. Geometry for calculation of effective volumes.

hence be undetected by the system. Since the kinetic energy of the decay products are high enough so the particles are in the minimum ionizing region, the 8 Mev corresponds to a path length of 5 cm. The decay process is isotropic so that if a particle is at a given radial distance from the wall the probability of a decay giving rise to a path length less than 5 cm can be calculated by computing the solid angle in which these paths lie. Consider the geometry shown in the lower triangle in Fig. 9. The radius of the sphere is denoted by r_s, the minimum detectable path by R, and the radial position of a particle by r. The angle β is determined by r_s, R, and r, and for a given r any paths lying inside the cone of angle β will be a path shorter than R. The fraction f of solid angle within the cone is seen to be

$$f(r)=[(R+r)^2-r_s^2]/4Rr. \tag{A4}$$

The effective number of particles N, which do not contribute to a detectable process is found by summing over the number of particles within a distance R of the wall times the fraction of a particle decay process which is not detectable. This yields the expression

$$N=\int_{r_s-R}^{r_s} 4\pi\rho r^2 f(r)dr, \tag{A5}$$

from which we find

$$N=\pi\rho(Rr_s^2-R^3/12). \tag{A6}$$

It is convenient to use r_s as a unit of length and express Eq. (A6) in terms of the ratio $x=R/r_s$. Using this designation, the dimensionless parameter $\eta(x)$ can be defined as

$$\eta(x)=x-x^3/12=N/\pi\rho r_s^3. \tag{A7}$$

The ratio of N to the total number of particles within the equivalent sphere can be expressed as

$$N/N_{\text{tot}}=3\eta/4. \tag{A8}$$

For this specific calculation it is reasonable to use

$r_s=38.7$ cm which gives the real surface area, in which case the value $R=5$ cm leads to $N/N_{\text{tot}}=9.3\%$. We therefore reduce the real number of protons in the tank by 9.3% to get the number effective for decay processes. The real number of protons is given by

$$N_{\text{tot}}=\pi b^2 h\rho_{\text{H}}, \tag{A9}$$

where ρ_{H} is the density of free protons. The value of ρ_{H} for decalin can be obtained from the density ρ (0.887 g/cm^3), the formula $C_{10}H_{18}$, and the molecular weight M (138.25 g/mole). ρ_{H} is therefore 7×10^{22} proton/cm^3. The volume of the liquid scintillator is 200 liters so that Eq. (A9) gives $N_{\text{tot}}=1.4\times10^{28}$ free protons. The effective number is then 9.3% less or 1.3×10^{28} free protons. The observed count rate was 18/421 counts per hour at energies greater than 8 Mev and 2/421 counts per hour at energies greater than 12 Mev. If these rates are taken as the highest possible rates actually occurring, they lead to lifetime limits of

$$2.5\times10^{25} \text{ yr } (E>8 \text{ Mev}),$$
$$2.0\times10^{26} \text{ yr } (E>12 \text{ Mev}).$$

However, for the decay modes in question, namely the mono-energetic charged particle modes, the kinetic energy release in each case is greater than 104 Mev. The fraction of isotropic decays depositing between 8 and 12 Mev can be computed to be 6% of the total. This means that if two high-energy counts are ascribed to decays, at most one of the low-energy counts should be ascribed to these decay modes and hence a total of only 3 counts with $E>8$ Mev. The lifetime limit in this view is then

$$\tau>1.3\times10^{26} \text{ yr } (E>8 \text{ Mev}).$$

These lifetime limits are then applicable to all the mono-energetic charged-particle decay modes listed in Table III, column 1, and the lifetime limits are so tabulated.

Bound proton, decay energy unique.—In order to calculate the number of bound protons inside the tank which can be effective for the decay process it is sufficient to multiply the effective free proton number of the last section by the ratio of bound protons to free protons in decalin, namely 10/3. In addition there is a contribution from the protons bound in the Fe nuclei of the shield material. For the decay modes under consideration a fixed range R in iron is associated with each mode. At any point in the shield the solid angle containing paths in iron shorter than R can be computed. Consider the geometry shown in the upper triangle in Fig. 9 where the shield inner radius is denoted by a. It is assumed that all paths within the solid angle determined by θ penetrate the inner tank and give a detectable signal. This is not geometrically exact since at value of r approximately equal to a, this angle θ gives a path which may not intersect the inner sphere and hence gives too large a value for θ. Since the air gap is small compared to r and a, this is not a serious overestimate and rapidly becomes unimportant at larger values of r. In the spirit of the approximations used this error will be neglected. With this geometry the expression for the fraction of solid angle containing admissible paths is

$$f(r)=[a^2-(r-R)^2]/4Rr, \tag{A10}$$

and the number of particles N effective for the decay process is

$$N=\pi\rho(Ra^2-R^3/12). \tag{A11}$$

This is just Eq. (A6) with a replacing r_s. By using the value of a as the unit of length and the value of ρ appropriate to iron, Eqs. (A6) and (A7) can be used to compute the effective number of protons in the shield for a given range R. The range is fixed by the type of particle and its energy, and is found for the particles from each decay mode from the appropriate momentum range curves.[19,20] The curves used are based on energy losses primarily due to radiation. In obtaining the range of the electrons (and photons) the simplest approximation to the cascade process was used, namely that an electron or a photon gives rise to a cascade pair after traversing one radiation length in iron. The cascade process stops when the particle energy drops below the critical energy, here about 21 Mev.

The total effective number of protons for a particular decay mode is then obtained by adding the effective number inside the tank (a constant number) to the effective number in the iron shield (a number depending on the decay mode energy release). The lifetime limits can then be calculated using Eq. (A1) with the appropriate count rate. The decay count rate to be used in calculating the lifetime is for pulses of energy greater than 12 Mev just the observed count rate of 2/421 counts/hr. However, the count rate for decay pulses of very low energy, between 8 and 12 Mev, should not be as large as the observed count rate for the following reason: In order that one of these decay modes give rise to a pulse of such a low energy the particle would travel only 7.5 cm through the detector tank, and hence the solid angle containing such a path is small. For the mesons having ranges in iron which vary from 17 to 30 cm the fraction of such decays is estimated to be between 2% and 1%. For electrons having shorter ranges in iron the estimate of the number of such decays is less than 3%. Again if two high-energy counts are ascribed to decay events, it is conservative to say that not more than one low-energy count is a decay event. Hence the lifetimes tabulated in Table III are computed using a decay rate of 3/421 counts/hr for the energy release in the detector above 8 Mev.

Bound proton, decay energy spectrum.—If the decay mode is such as to give more than two particles, each particle will have a possible range of energies. For the

[19] B. Rossi, *High-Energy Particles* (Prentice-Hall, Inc., Englewood Cliffs New Jersey, 1952), p. 44.

[20] W. Heitler, *The Quantum Theory of Radiation* (Oxford University Press, New York, 1954), p. 376.

simplest cases where one charged particle and two neutrinos are emitted, a spectrum for the charged particle can be readily computed. The spectrum can then be found in terms of relative number of particles as a function $S(R)$ where R is the range in iron, and then the effective number of protons in the shield can be expressed as

$$N=\int_0^{R_0} S(R)\pi\rho a^3\eta(x)dR \Big/ \int_0^{R_0} S(R)dR, \quad \text{(A12)}$$

where $x=R/a$, and R_0 is the maximum range.

The spectrum for one of the simple decay modes will be used in an example of this procedure. Consider the decay mode,

$$p^+ \rightarrow \mu^+ + \nu + \bar{\nu}. \quad \text{(A13)}$$

The spectrum can be computed on the basis of phase space arguments[21] and is

$$S(p)dp \propto dp\left\{\frac{2p^4}{(m_pc)^4}-\frac{6p^2[p^2+(m_\mu c)^2]^{\frac{1}{2}}}{(m_pc)^3} + \frac{3p^2}{(m_pc)^2}\left(1+\frac{m_\mu^2}{m_p^2}\right)\right\}, \quad \text{(A14)}$$

where p is the momentum of the charged product, m_p is the proton mass, and m_μ is the muon mass. This spectrum is plotted as a function of range in iron in Fig. 10. When the spectrum of Fig. 10 is used in Eq. (A12), numerical integration gives a value for the effective number of protons in the shield of 2.5×10^{29}. The effective number of protons inside the scintillator is essentially the same as that computed for the bound proton, unique energy decay case 0.5×10^{29}, since the number of decay muons with ranges less than 5 cm is only 1% of the total number. The lifetime for this mode can then be computed using the sum of these effective numbers 3.0×10^{29} as the possible source of decay events. From the spectrum it can be ascertained that less than 1% of the muons have kinetic energies less than 12 Mev, so that any contribution to the count rate from such events can be neglected. The estimated fraction of paths giving small pulses which was used in arriving at the decay count rate for mono-energetic modes should therefore be appropriate to the possible muon decays. Hence the decay count rate from the low-energy events is taken as 1/421 counts/hr. The total count rate, 3/421 counts/hr gives a lifetime for this mode of decay of 3×10^{27} years.

The same procedure can be used to compute the lifetime for the mode in which a proton decays into an electron plus two neutrinos. That spectrum is given by Eq. (A14) if m_μ is set equal to m_e or effectively zero.

[21] E. Fermi, *Elementary Particles* (Yale University Press, New Haven, Connecticut, 1951), pp. 44–47.

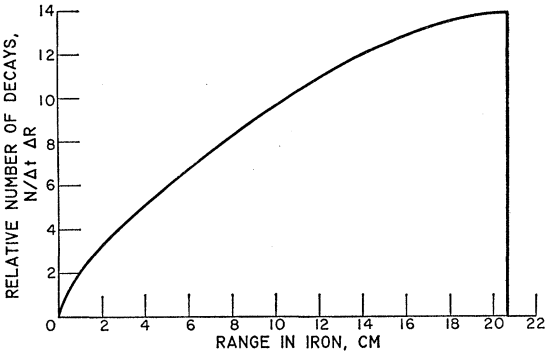

FIG. 10. Range spectrum of muons from decay mode $p^+ \rightarrow \mu^+ + \nu + \bar{\nu}$.

Further in the cases where a charged lepton plus an electron pair are the decay products, the procedure is still a good approximation for most of the spectrum. The spectral shape, which in this approximation is determined only by a statistical factor, is affected by the finite electron rest mass only at the high-energy end, in a region having an energy spread of a few Mev.

Calculation of Bound Neutron Lifetime

Unique decay energy.—All such decay modes listed in Table III will result in contributions from decaying neutrons bound in nuclei in the liquid scintillator and in the iron shield. Since two charged particles are given off for the two-particle decay modes, no correction for edge effects inside the scintillation detector is necessary. Also in some cases the range of one particle is much larger than that of the other so only contributions from the long-range particles originating in the shield are used in computing the lifetimes. The computations are otherwise similar to those used for computing the bound proton monoenergetic decay lifetimes.

Decay energy spectrum.—The computations for lifetimes of decay modes leading to an energy spectrum of a charged particle are based on the same considerations used for the proton decays with energy spectra. The adjustment of the decay count rate (for the energy releases between 8 and 12 Mev) from the observed count rate is also based on the considerations used for proton decay modes.

Modes Releasing 250-Mev Kinetic Energy

The lifetime limits for the decay modes listed in Table IV are computed by assigning a unique energy 250 Mev to the listed decay product, and then using the procedure detailed in the previous subsection of this appendix titled *Bound proton, decay energy unique.* The sources are taken to be either protons or all nucleons.

ACKNOWLEDGMENTS

The authors wish to thank the Morton Salt Company for providing hospitality and facilities at their Fairport Harbor Mine, the Republic Steel Corporation for their gift of the shielding material, A. A. Hruschka for his contribution to the design and fabrication of the detectors, Professor T. L. Jenkins for valuable discussions, Mrs. C. C. Giamati for assistance in data reduction and film reading, and W. R. Kropp for help in taking data at Case Institute.

PHYSICAL REVIEW VOLUME 126, NUMBER 6 JUNE 15, 1962

$\pi^-+p\rightarrow\pi^0+n$ Charge Exchange Cross Sections at 20.7 and 31.0 Mev

K. MIYAKE,* K. F. KINSEY, AND D. E. KNAPP†
The University of Rochester, Rochester, New York

(Received November 21, 1961)

A measurement has been made of the differential and total cross sections at 31.0 Mev and the total cross section at 20.7 Mev for the reaction $\pi^-+p\rightarrow\pi^0+n$. A thin-walled liquid hydrogen target was used. The gamma telescopes used a Čerenkov counter to identify the conversion electrons and a thin-lead converter to avoid complications from cascade processes. The angular distribution in mb/sr at 31.0 Mev is: $d\sigma/d\Omega=(1.00\pm0.02)[(0.51\pm0.04)-(0.61\pm0.11)P_1(\cos\theta)+(0.12\pm0.36)P_2(\cos\theta)]$. The total cross sections at 31.0 and 20.7 Mev are 6.5 ± 0.5 and 5.4 ± 0.4 mb, respectively. The data are also analyzed in terms of the phase shifts α_{ij}. Assuming that the S-wave phase shifts extrapolate to zero pion energy as $\alpha_i=a_i\eta$, where η is the pion momentum in the c.m. system in units of $m_\pi c$, the quantity $(a_1-a_3)=0.27\pm0.02$. This agrees with Hamilton and Woolcock's prediction from photoproduction and the Panofsky ratio $(a_1-a_3)=0.245\pm0.01$. There are theoretical and experimental grounds for a nonlinear behavior of α_3 and α_1, which should improve the agreement.

I. INTRODUCTION

THE pion-proton interaction has been studied extensively since the advent of reasonably intense pion beams. At low pion energies (below ~200 Mev), the predominant features of the scattering have been satisfactorily explained in terms of a resonance in the $T=\frac{3}{2}$, $J=\frac{3}{2}$ state at ~170 Mev. However, because of the dominance of this resonance, the smaller phase shifts have been more difficult to measure and there still remain problems concerning their behavior, especially at low energy. In particular, the quantity $(\alpha_1-\alpha_3)/\eta$ (where α_i are the S-wave phase shifts for the two isotopic spin states and η is the center-of-mass pion momentum in units of $m_\pi c$) can be calculated, in the limit of zero energy, from low energy scattering data and independently, from the Panofsky ratio and pion photoproduction data. There has been some discrepancy between the results of these two ways of calculating this quantity.

The charge exchange reaction, $\pi^-+p\rightarrow\pi^0+n$, provides a sensitive determination of this quantity, and furthermore, the Coulomb corrections to the phase shifts, important for the elastic scattering at these energies, are not present. This reaction has been measured at this laboratory by Spry[1] and by Roberts and Tinlot.[2,3] The experimental uncertainties in these measurements are considerably greater than for the presently available data on the elastic scattering processes near 30 Mev.[4–7] In this paper we report a measurement of the total and differential cross sections at 31 Mev and a total cross section measurement at 20.7 Mev for the charge exchange reaction. There is now a complete set of data of comparable accuracy for all of the observable pion-proton interactions at 31 Mev. The value of $(\alpha_1-\alpha_3)/\eta$ obtained is shown to be in reasonable agreement with the prediction from the Panofsky ratio, etc.

The technique of the present experiment differs from the previous work[1–3] in three respects:

(1) A thin lead converter (about 0.3 radiation lengths) was used to avoid complications arising from cascade processes.

(2) A Čerenkov counter was used to detect and identify the conversion electrons. This eliminated a great deal of the background.

(3) The pions were scattered by a thin-walled liquid-hydrogen target. These improvements contribute to the higher accuracy of the experiment and should introduce a different set of possible systematic errors.

* Present address: University of Kyoto, Kyoto, Japan.
† Present address: Douglas Aircraft Corporation, Santa Monica, California.
[1] W. Spry, Phys. Rev. **95**, 1295 (1954).
[2] A. Roberts and J. Tinlot, Phys. Rev. **90**, 951 (1953).
[3] J. Tinlot and A. Roberts, Phys. Rev. **94**, 137 (1954).
[4] W. B. Johnson and M. Camac, Bull. Am. Phys. Soc. **3**, 197 (1958).
[5] S. W. Barnes, B. Rose, G. Giacomelli, J. Ring, K. Miyake, and K. Kinsey, Phys. Rev. **117**, 226 (1960).
[6] S. W. Barnes, H. Winick, K. Miyake, and K. Kinsey, Phys. Rev. **117**, 238 (1960).
[7] G. Giacomelli, Phys. Rev. **117**, 250 (1960).

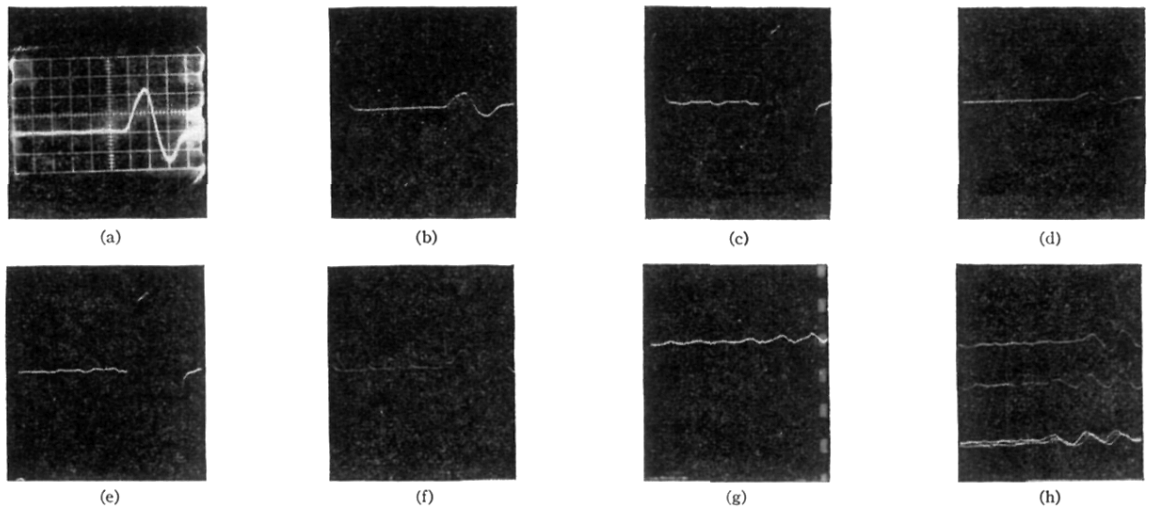

FIG. 7. Typical oscilloscope traces. The sweep speed is 1 μsec/cm. The left-hand pulse at the beginning of the sweep is the Čerenkov pulse. The scintillation detector pulse is delayed 6 μsec with respect to start of sweep. (a) Calibration trace from pulse generator. (b), (c) Cosmic-ray events. (d) Scintillation pulse of 12-Mev energy unaccompanied by a Čerenkov pulse. (e) Scintillation pulse of energy greater than 150 Mev unaccompanied by a Čerenkov pulse. (f), (g), (h) Noise pulses.